A Study on Sodium Effects on the Mechanical Properties of Ferritic-Martensitic Steels

Sang Hun Shin [a], Jun Hwan Kim [b], Ji Hyun Kim [a*]
[a]*Scholl of Mechanical and Nuclear Engineering, Ulsan National Institute of Science and Technology (UNIST)*
100 Banyeon-ri, Eonyang-eup, Ulju-gun, Ulsan 689-798, Republic of Korea
[b]*Advanced Fuel Development Division, Korea Atomic Energy Research Institute (KAERI)*
P.O. Box 105, Yuseong, Daejeon 305-600, Republic of Korea
[*]*Corresponding author: kimjh@unist.ac.kr*

1. Introduction

A sodium-cooled fast reactor (SFR) that uses fast neutrons as a fission process is considered one of the most probable candidates in next generation reactors [1]. As an SFR core experiences high temperatures (650℃) and neutron doses (200 dpa), ferritic-martensitic steel, especially HT9 steel containing 12% Cr, is being considered due to its superior dimensional stability against high-energy neutron irradiation [2]. On the other hand, ASTM A192 Gr.92 (9Cr-0.5Mo-2WVNb) steels are known to have higher creep resistance than HT9 (12Cr-1Mo-VW) steel which is a widely used cladding material in SFRs [3].

The irradiation properties are important for cladding materials such as steel. The irradiation properties of ASTM A192 Gr.92 have been compared to HT9. After irradiation to 35 dpa at 420℃, at the Fast Flux Test Facility (FFTF), swelling of the reduced-activation 9Cr-2WV and 9Cr-2WVTa steels and the conventional 9Cr-1Mo-VNb and 12Cr-1Mo-VW steels was estimated by transmission electron microscopy (TEM) to be 0.2%, 0.33%, 0.85%, and 0.007%, respectively [4]. The irradiation creep coefficient for neutron-irradiated steels is 2×10^{-7} MPa^{-1} dpa^{-1} for HT9 at 425–500℃ with 50 dpa (EBR-II) [5], 5×10^{-7} MPa^{-1} dpa^{-1} for HT9 at 440–500℃ with 14 dpa (EBR-II) [6], and 1.5×10^{-7} MPa^{-1} dpa^{-1} for JLF1 (9Cr-2WMnVTa) at 390–410℃ with 36 dpa (FFTF) [7]. An average value near 5×10^{-7} MPa^{-1} dpa^{-1} is a good estimate for such ferritic/martensitic steels.

In this study, ASTM A192 Gr.92 steels were exposed to liquid sodium at 650℃ for 1583 h and 3095 h and evaluation of the microstructure as well as the mechanical properties using ring hoop tensile tests and ring hoop creep tests were conducted.

The objective of this study is to evaluate the microstructure and mechanical properties of ferritic-martensitic steel (ASTM A192 Gr.92) that has been exposed to a high-temperature sodium environment.

2. Experiments

For the comparison of an ASTM A192 Gr.92 cladding tube and a HT9 cladding tube, ring tensile tests were carried out at room temperature and 650℃ on as-received specimens. A compatibility test facility was manufactured.

The facility was designed to flow liquid sodium with natural circulation caused by the temperature control. Detailed parameters regarding the facility have been published elsewhere [8]. A compatibility test of the ferritic-martensitic cladding tube was carried out. The test cladding tube was an ASTM A192 Gr.92 cladding tube with a 7 mm outer diameter and 0.6 mm thickness. The tube was tested in 650℃ liquid sodium for a maximum of 3095 h, where the first cladding tube was exposed to sodium for 1583 h and was then interrupted to insert another cladding tube to continue for an additional 1512 h. In addition to the sodium compatibility test, the cladding specimen was aged for comparison. The cladding tubes were aged in an argon environment at 650℃ for 1601 h and 2973 h.

After the compatibility test, the cladding was cut to observe the microstructure (for the carbon extracted replica) and also machined as a ring specimen with a 1.84 mm gauge length and a 1.25 mm width. Ring tensile tests were performed at room temperature, 300℃, 400℃, 500℃, and 650℃ at a strain rate of 0.001 s^{-1}. Ring creep tests were also performed at 650℃ with as-received specimens.

3. Results and discussion

Fig. 1 shows the load-displacement curve of as-received Gr.92 and HT9 ring specimens carried out at room temperature and 650℃ with a 0.001 s-1 strain rate. HT9 tubes showed longer displacement at room temperature and 650℃. At room temperature, the maximum load of both steels is similar and at 650℃, Gr.92 showed a higher maximum load than HT9.

After the compatibility test, the ring specimens were cut from the Gr.92 cladding tube to carry out ring tensile tests at room temperature and high temperatures (300℃, 400℃, 500℃, and 650℃) with a 0.001 s-1 strain rate as well as ring creep tests. Typical load-displacement curves obtained are shown in Fig. 2 (a). Extensometers were not available which could span the gauge lengths of the ring specimens, so the cross head displacement had to be used to assess the strain of the specimens.

Table I. Chemical composition of the test material

	C	Si	Mn	Cr	Ni	Mo	W	V
HT9	0.19	0.14	0.49	12.05	0.48	1.00	0.49	0.30
Gr.92	0.087	0.21	0.41	8.69	0.13	0.38	1.62	0.18

At room temperature, the maximum cross-head displacement recorded was 0.654 mm for the as-received specimen, 0.765 mm for the specimen aged in argon for 1601 h, 0.569 mm for the specimen aged in argon for 2973 h, 0.881 mm for the specimen exposed to sodium for 1583 h, and 0.681 mm for the specimen exposed to sodium for 3095 h, thus resulting in 35.5%, 41.6%, 30.9%, 47.9%, and 37.9% elongation to failure, respectively. Also, the maximum load was attained at an elongation of 33.1%, 32.8%, 26.4%, 32.6% and 30.9%, respectively. Thus the final 2.4%, 8.8%, 4.5%, 15.3% and 7% elongation, respectively, were due to necking. Since the area under the force-cross head displacement curve indicates the fracture energy, the energy associated with these tests were calculated by numerical integration using the trapezoid rule and were found to be 0.591 J, 0.605 J, 0.399 J, 0.707 J, and 0.484 J, respectively. All argon-aged specimens and Na-exposed specimens showed a lower maximum load compared with the as-received specimen. Na-exposed specimens showed larger strain than argon-aged specimens. The data is summarized in Table II where A.R, Ar, and Na represent the as-receives specimen, argon aging for a given time, and Na exposure for a given time, respectively. In Fig. 2 (b), the maximum load applied to all specimens decreased with increasing temperature with the highest applied to the as-received. A sharp transition in behavior occurred at around 400℃ with the elongation recovering in this temperature region [9, 10]. The specimen exposed to sodium for 1583 h showed the highest elongation as shown in Fig. 2 (c).

Fig. 3 shows the TEM images of the extraction replicas for the precipitates in the as-received specimen. Nano-sized precipitates were observed in the as-received specimen. Their representative composition was determined to be (in at%) 7.6Cr-43.4V-37.8N-1.9Nb (A1) indicating V-rich MX-type (M = Nb, V, Cr, W and X = C, N) carbonitride and 31.1Fe-58.5Cr-6.6W-1.2V-1.4Mo-1.1Mn (A2) indicating a complex compound of $(Cr, Fe, W, Mo)_{23}C_6$.

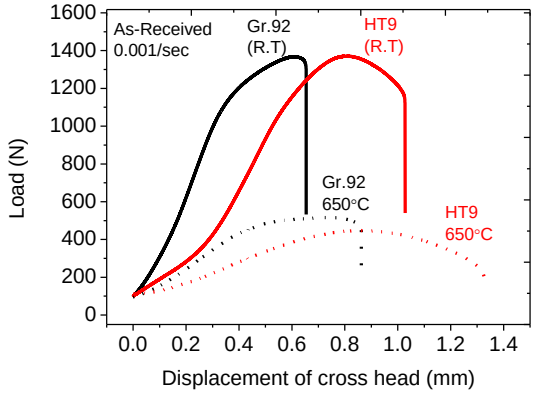

Fig. 1. Load-displacement curves of ring hoop tensile tests of as-received (A.R), Gr. 92, and HT9 specimens carried out at room temperature (line) and at 650℃ (dotted line).

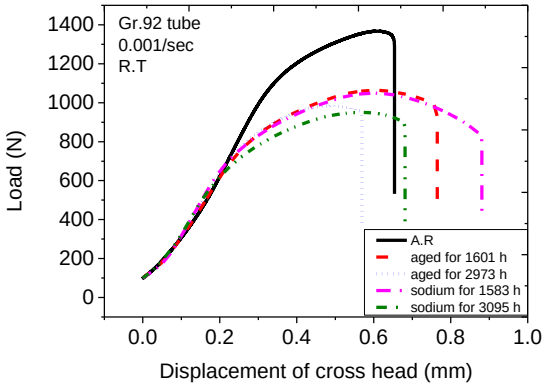

(a)

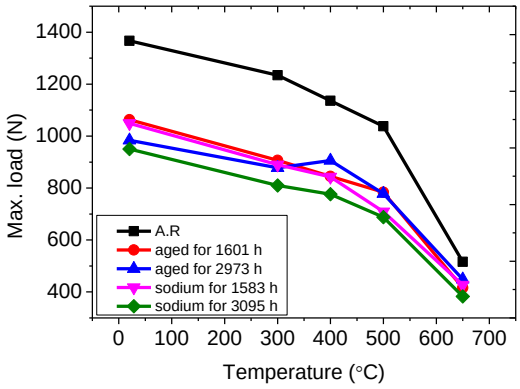

(b)

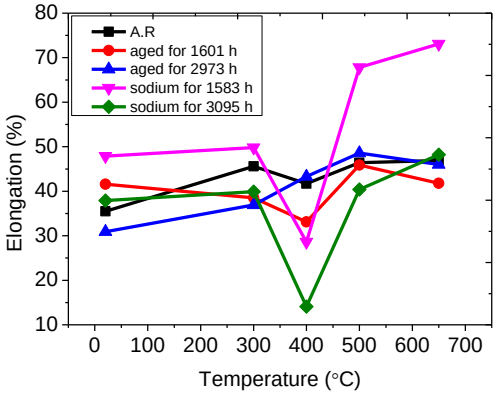

(c)

Fig. 2. (a) Load-displacement curves of ring hoop tensile tests of as-received (A.R), aged (for 1601 h and 1973 h), and Na aged Gr. 92 (1583 h and 3095 h) specimens carried out at room temperature, temperature dependency of (b) maximum load, and (c) elongation of each specimen.

The $M_{23}C_6$ carbides were mainly detected in the prior-austenitic grain boundaries, but occasionally in the subgrains and lath boundaries. The MX precipitates were usually found in the lath and lath boundaries. The mean size of the precipitates was 47 nm. TEM images of the extraction replicas for the precipitates in the specimens that were exposed to sodium are shown in Fig. 4 (a) and (b). The compositions of the precipitates

were largely composed of (Cr, Fe, W, Mo)$_{23}C_6$. The $Cr_{23}C_6$ carbides were detected mostly in the specimens which were exposed to sodium environment. The mean sizes of these precipitates were 113 nm for 1583 h and 218 nm for 3095 h exposure. TEM images of the extraction replicas for the precipitates in the specimens which were aged in an argon environment are shown in Fig. 4 (c) and (d). The Laves phase (Fe_2W) was mainly detected in these specimens. The mean size of the precipitates was 143 nm for 1601 h and 171 nm for 2973 h exposure.

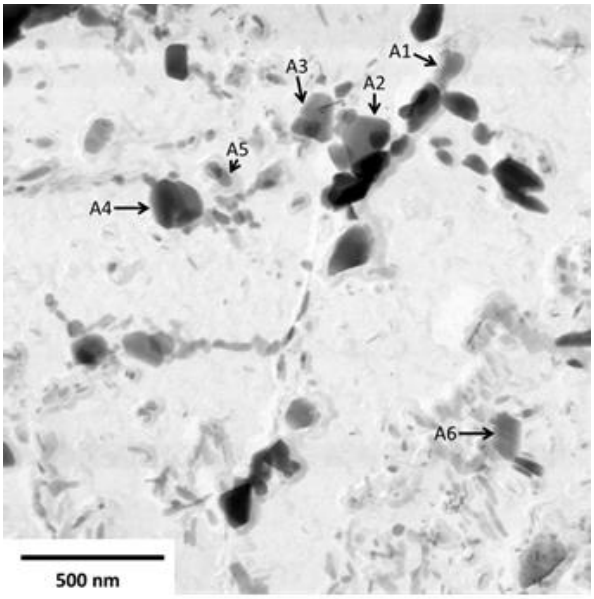

Fig. 3. TEM image of the as-received Gr. 92 specimen

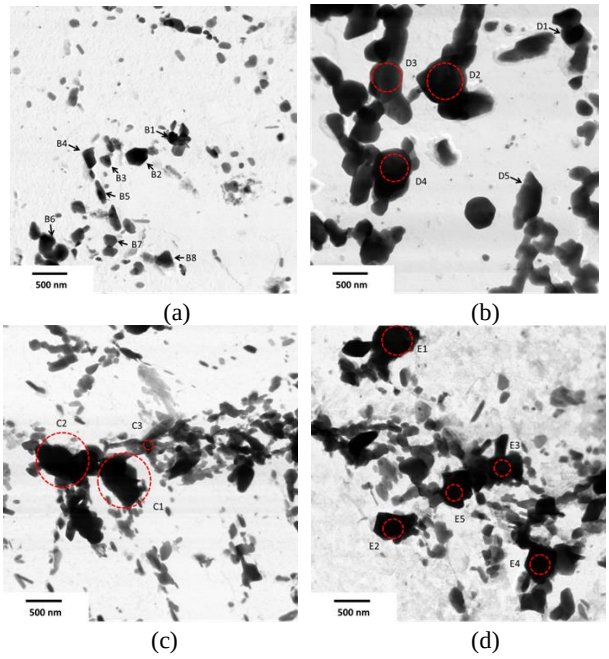

Fig. 4. TEM images of ring specimens exposed to (a) 650℃ sodium for 1583 h, (b) 650℃ sodium for 3095 h, (c) 650℃ argon environment for 1601 h, and (d) 650℃ argon environment for 2973 h.

Table II. Summary data for the ring tensile tests

Temp.	Samples	Elongation to failure (%)	Maximum load (N)
R.T	A.R	35.5	1367
	Ar (1601 h)	41.6	1063
	Ar (2973 h)	30.9	984
	Na (1583 h)	47.9	1049
	Na (3095 h)	37.9	950
300℃	A.R	45.6	1234
	Ar (1601 h)	38.5	907
	Ar (2973 h)	36.9	878
	Na (1583 h)	49.8	890
	Na (3095 h)	39.9	810
400℃	A.R	41.7	1136
	Ar (1601 h)	33.1	845
	Ar (2973 h)	43.3	906
	Na (1583 h)	28.6	843
	Na (3095 h)	14.1	776
500℃	A.R	46.4	1038
	Ar (1601 h)	45.9	784
	Ar (2973 h)	48.6	778
	Na (1583 h)	67.8	709
	Na (3095 h)	40.4	688
650℃	A.R	46.9	516
	Ar (1601 h)	41.8	416
	Ar (2973 h)	46.0	449
	Na (1583 h)	73.1	427
	Na (3095 h)	48.2	383

To determine the liquid sodium effect in this study, two processes, decarburization and depleted chromium from the metal into the liquid sodium, are discussed. In sodium exposed specimens, mainly $M_{23}C_6$ precipitates were observed and the Laves phase was not observed. At the surface of these specimens, chromium depletion and decarburization were observed. With a computational thermodynamic program (JMatPro 7.0) the sensitivity of the precipitates as function of C content was plotted in Fig. 5.

On the basis of the chemical composition of Gr.92, the first case showed early exposure time with 7 wt% Cr where 1.69 wt% Cr is depleted into the liquid sodium. As C content decreases the amount of $M_{23}C_6$ also decreases while the amount of the Laves phase increases, as shown in Fig. 5 (a). In the second case where 4.69 wt% of Cr is depleted with longer simulated exposure time, no Laves phase was thermodynamically formed except for the case of 0.01 wt% C. In this case, the $M_{23}C_6$ precipitate exists between 0.087 wt% and 0.05 wt% as shown in Fig. 5 (b).

In this study, the decarburization zone was measured to be about 60 μm for both sodium exposed specimens (1583 h and 2973 h). As summarized in Table. II, the argon aged specimens showed higher maximum load than that of Na exposed specimens with similar aging times.

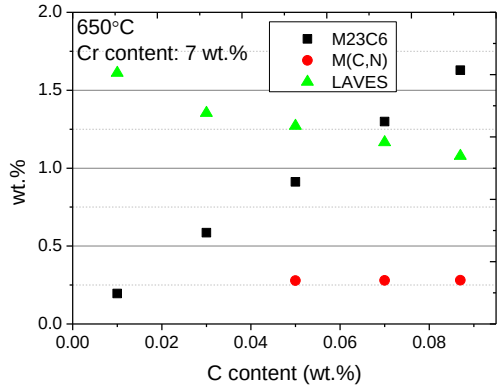

(a)

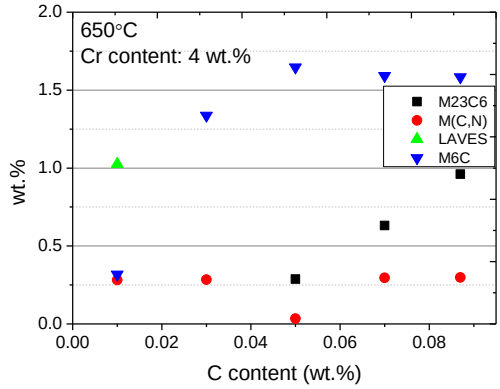

(b)

Fig. 5. Sensitivity of the precipitates as function of carbon concentration in the matrix with a given concentration of chromium

Fig. 6 draws a comparison the ring hoop creep properties of ferritic-martensitic steels (FMS) tested in this study with other FMS from literature [11-13]. The FMS creep properties appear to be similar to ones of the FMS, as measured from the literature.

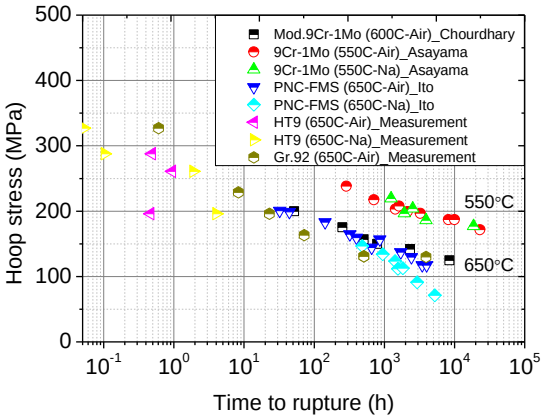

Fig. 6. Comparison of the creep lifetime of the HT9 and Gr.92 steels with that of FMS from literature.

Little information is available on the creep rupture properties of FMS exposed to high temperature sodium. K. Natesan et al., [14] revealed that little difference in creep strength between as received and sodium-exposed specimens of mod. 9Cr-1Mo. No effect of pre-sodium exposure (associated carbon gain/loss) was observed after 5000 h exposure to sodium at 500-550°C.

4. Conclusions

In order to investigate the effect of the aging process on the precipitates and the mechanical properties of Gr. 92 steel, specimens were exposed to 650°C liquid sodium and aged in a 650°C argon environment for a given time. V-rich MX-type carbonitride and $M_{23}C_6$ were found in the as-received specimen. In the specimens which were exposed to sodium, mainly $Cr_{23}C_6$ was observed while the Laves phase was mainly observed in the specimen that was aged in an argon environment.

The maximum load of Gr. 92 steel that was exposed to the liquid sodium environment was lower than that of the argon aged specimens. It is believed that the behavior of the specimens exposed to sodium is affected by decarburization and chromium depletion (caused the composition of $M_{23}C_6$ precipitates in the matrix).

Ring hoop creep tests are under progress.

ACKNOWLEDGEMENT

This work was financially supported by the 'SFR Cladding Development Project' supported by the National Nuclear R&D program in the Ministry of Science, ICT and Future Planning (MSIP).

REFERENCES

[1] J.H. Kim et al., J. Nucl. Mater. **433** (2013) 112.
[2] F. Delage et al., J. Nucl. Mater. **441** (2013) 515.
[3] F. Masuyama, in: Advanced Heat Resistant Steels for Power Generation, Eds. R. Viswanathan and J. Nutting (The Inst. of Materials, London, Book **708**, 1999) 99.
[4] J.J. Kai and R.L. Klueh, J. Nucl. Mater. **230** (1996) 116.
[5] B.A. Chin, in: Topical Conference on Ferritic steels for Use in Nuclear energy Technologies, Eds. J.W. Davis and D.J. Michel (The Metallurgical Society of AIME, Warrendale, PA, 1984) 593.
[6] R.J. Puigh and G.L. Wire, , in: Topical Conference on Ferritic steels for Use in Nuclear energy Technologies, Eds. J.W. Davis and D.J. Michel (The Metallurgical Society of AIME, Warrendale, PA, 1984) 601.
[7] A. Kohyama, Y. Kohno, K. Asakura, M. Yoshino, C. Namba, C.R. Eiholzer, J. Nucl. Mater. **212-215** (1994) 751.
[8] J.H. Kim et al., Kor. J. Met. Mater., **48**, 410 (2010)
[9] P. Skeldon et al., Corros. Sci. **36** (1994) 593.
[10] J.P. Hilditch et al., Corros. Sci. **37** (1995) 445.
[11] B.K. Choudhary et al., J. Nucl. Mater. **412** (2011) 82.
[12] T. Ito et al., Research Report of the Japan Atomic Energy Agency PNCTN941093-045 (1993)
[13] T. Asayama et al., J. Press. Vess. Technol. **123** (2011) 49.
[14] K. Natesan et al., J. Nucl. Mater. **392** (2009) 243.